Resonant Neutron Capture in ^{175}Lu†

O. A. Wasson and R. E. Chrien
Brookhaven National Laboratory, Upton, New York 11917
(Received 27 March 1970)

A study of the neutron-capture reaction mechanism for radiative capture of resonant-energy neutrons has been made for ^{175}Lu$(n,\gamma)^{176}$Lu. The statistical distribution of the partial radiation widths over 11 neutron resonances is inconsistent with a χ^2 distribution with one degree of freedom. No correlations are observed between the γ-ray partial widths and the reduced neutron widths of either the capturing or final states. Neither is there any significant correlation among the individual γ-ray widths. Such facts indicate that neither channel capture nor doorway states contribute strongly to the neutron-capture process in the region above the neutron binding energy. However, there is a small but significant departure from a purely statistical compound-nuclear process. Final states unreported in previous experiments are observed. In addition, the spins of 11 resonances, as well as limitations on the spins of the low-lying final states are determined.

I. INTRODUCTION

The measurement of the radiative transitions following slow neutron capture has recently produced considerable insight into the neutron-capture reaction mechanism. Evidence has been seen for the competition between direct and compound-nuclear reactions, while correlations between the radiative transition strengths and the reduced neutron widths of initial and final states have been interpreted in terms of single-particle (or valence-neutron) transitions or the influence of three-quasiparticle doorway states in the capture process.

One means of studying the neutron reaction mechanism is from the distribution of partial radiation widths and the correlations between these partial widths and various nuclear-structure parameters such as the reduced neutron widths. It was first proposed by Porter and Thomas[1] that the variation of the partial radiation widths from the highly excited states above the neutron binding energy is quite broad, following a χ^2 distribution with one degree of freedom. This distribution results from the assumed random nature of the radiative-decay amplitudes. For many nuclei,[2-5] the distribution of partial widths is consistent with one degree of freedom. However, there is recent evidence in some nuclei for a narrower distribution which is characterized by a larger number of degrees of freedom.[6,7] The effects of various processes on the statistics of the radiative widths is discussed by several authors.[8-12]

Investigations of the correlations between partial radiation widths and the reduced neutron widths of both capturing and final states determine the importance of doorway states and channel capture in the reaction mechanism.[9,13-17] Although there are numerous examples of correlations between γ-ray widths and reduced neutron widths of final states as well as capturing states,[18] strong γ-ray correlations with both the capturing-state and final-state reduced neutron widths in the same nucleus have not been observed.

The purpose of the present work is to measure the distribution of partial radiation widths and the various correlations in order to search for specific nuclear-structure effects in radiative neutron capture in lutetium. In the process additional information on the resonance spins and spectroscopy of the final states is obtained.

The existing data on the nuclear properties of ^{176}Lu is far from complete. Although the energies and neutron widths of the resonances in ^{175}Lu are known,[19-21] the resonance spins were previously unknown. The most recent thermal-neutron-capture γ-ray measurements were done by Minor *et al.*,[22] who used an isotopically enriched sample as well as γ-γ coincidences. A revised decay scheme with spins and parities, as well as certain Nilsson rotation bands, was proposed. This revision made use of the (d,p) experiments of Struble and Sheline,[23] who measured the relative intensity of the proton groups at three angles and deduced spin and configuration assignments on the basis of calculations from a rotational model. Previous recent work also included the precision low-energy γ-ray measurements[24] and conversion-electron[25] measurements from thermal-neutron capture.

II. EXPERIMENTAL DETAILS

The experiment was performed using the 22- and 48-m flight paths of the fast-chopper facility[26] at the high flux beam reactor at Brookhaven National Laboratory. The γ rays from neutron capture in the sample were detected in a Ge(Li) detector. The flight time and pulse size of each event were recorded on magnetic tape and consequently pro-

cessed at the central computer facility in a manner described in a previous publication.[27] The main part of the experiment was done using the 48-m flight path. A 4-cc Ge(Li) planar diode was placed behind a 12-in.-thick Pb shadow cone in the center of the neutron beam. The 100-g sample of Lu_2O_3 powder with normal isotopic abundance was placed in an aluminum annulus surrounding the detector. This geometry allows the maximum solid angle to be subtended by the detector. A total of 163-h beam time was used for this part of the experiment, using a chopper speed of 6000 rpm. The neutron energy region below 2 eV was covered in a second experiment at the 22-m flight path. The sample was placed in the middle of the neutron beam with the axis of the Ge(Li) detector oriented at 90° to the beam and placed out of the beam. The chopper speed was 1500 rpm with a running time of 24 h. The neutron energy region extended from 0.92 to 1.8 eV and included the 0.14- and 1.57-eV resonances in the low-abundance isotope ^{176}Lu as well as a "thermal" spectrum which is dominated by the ^{176}Lu(n,γ) reaction. Only the high-energy γ rays, which deposited more than 3 MeV in the detector, were recorded in the above experiment.

Several months later a 240-g sample of Lu_2O_3 enriched to 99.93% ^{175}Lu was received. Another low-chopper-speed run with a 37-cc detector was done. For this sample the contribution of the ^{176}Lu impurity to the thermal capture cross section was calculated to be about 2%. This sample was also run at the 48-m flight path in regular geometry for 16 h to obtain the low-energy γ-ray spectra from the higher-energy resonances.

III. EXPERIMENTAL RESULTS

The γ-ray counting rate for those events which deposit more than 3000 keV of energy in the detector is shown as a function of neutron flight time in Fig. 1. The three resonances due to the ^{176}Lu impurity are indicated by the dashed vertical lines, while the ^{175}Lu resonances are indicated by the solid vertical lines. It is clear that 11 resonances in $Lu^{175}(n,\gamma)$ are resolved. The neutron energy intervals selected to obtain γ-ray spectra are indicated by the horizontal bars.

The resultant γ-ray spectra are shown in Figs. 2–4. Because of the small Ge(Li) detector size, the peaks in the γ-ray spectra are mostly due to the two-photon escape peaks following pair production; hence the horizontal scale labels the incident γ-ray energy, which is 1022 keV more than the energy deposited in the detector. The highest-energy γ ray observed has an energy of 6053.8 keV and is labeled 1 in the 49.5- and 50.2-eV spectrum. The energy resolution of this γ-ray for the sum of eight days of data taking is 7.5 keV full width at half maximum. The γ-ray intensities vary greatly from resonance to resonance, which is typical of most resonance capture γ-ray spectra. The γ-ray spectra are so complex that many γ rays are not resolved for energies less than 5000 keV, even with the resolution of 7.5 keV. This spectral complexity is shown in Fig. 5 which contains the combined spectrum of 18 resonances. Below 5000 keV the peaks are not due to individual γ rays but to the sum of several γ rays. Much higher resolution is required to separate individual lines in this region. Throughout the remainder of this paper, the region below 5000 keV will be called the continuum region. Only that region above 5300 keV is used to analyze individual γ rays. The γ-ray intensities in the summed spectrum demonstrate large variations, but much less than in the individual spectra.

The high-energy γ-ray energies and intensities are listed in Table I. The first column numbers the γ ray; the second lists the γ-ray energies; the third lists the excitation energy of the final state, assuming that the γ ray is a primary transition from the capturing state; the fourth lists the final-state spin; while the remaining columns contain the γ-ray intensities. The last column contains the average γ-ray intensity for 15 resonances. Both members of the two unresolved resonances near 30 and 50 eV are assigned equal weight in

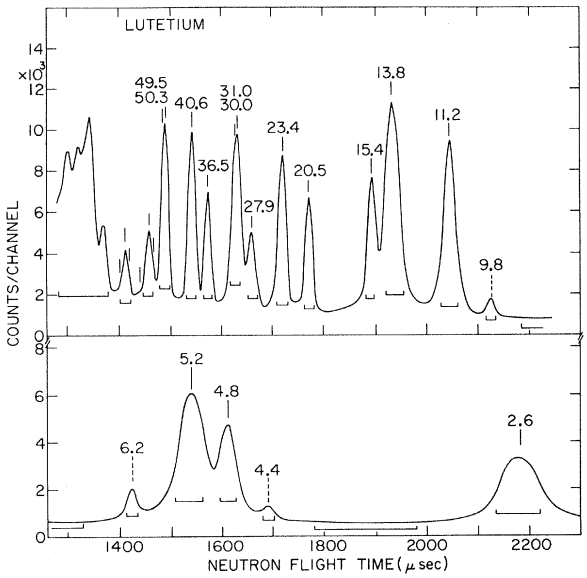

FIG. 1. Time-of-flight spectrum for those events which deposit more than 3000-keV energy in the detector. The resonances due to ^{175}Lu and ^{176}Lu target nuclei are indicated by solid and dashed vertical lines, respectively, using the neutron energies from Ref. 21. The horizontal bars indicate the intervals selected to obtain γ-ray spectra.

evaluating the average. The standard deviations for the statistical uncertainty in the γ-ray intensities are given in parentheses. For the average intensity the quantity in parentheses represents the deviation due to the finite size of the statistical sample rather than the uncertainty in the experimental measurement. The intensities greater than twice the standard deviation are underlined, which is the criterion used to establish the existence of the γ ray. The negative numbers result from the peak-fitting program.

A. γ-Ray Energy Calibration

The γ-ray energies are determined relative to the iron background γ rays observed in the off-resonance region. The electronic gain is determined by the separation of the single-escape and double-escape peaks of the strong γ rays. Using as a standard the value of 6018.4 ± 8.8 keV for the iron γ-ray energy quoted by Greenwood[28] yields an energy of 6053.8 ± 1.2 keV for the highest-energy lutetium γ ray. Combining this with the excitation energy of 239.4 ± 0.1 keV for the corresponding final state as deduced by Minor *et al.*,[22] yields a neutron binding energy of 6293.2 ± 1.2 keV for the neutron binding energy. This compares with the value of 6293 ± 4 keV reported by Minor *et al.*[22] and is also consistent with the value of 6294.6 ± 8.0 keV deduced from the (d,p) experiments.[23] The excitation energies listed in Table I are measured relative to the 239.4-keV state. The listed error of 1.0 keV includes only the statistical errors in deducing the energy difference between the above reference state and the particular final state.

B. γ-Ray Intensities

The usual technique is used to determine the γ-ray intensity. It is assumed that the total counts

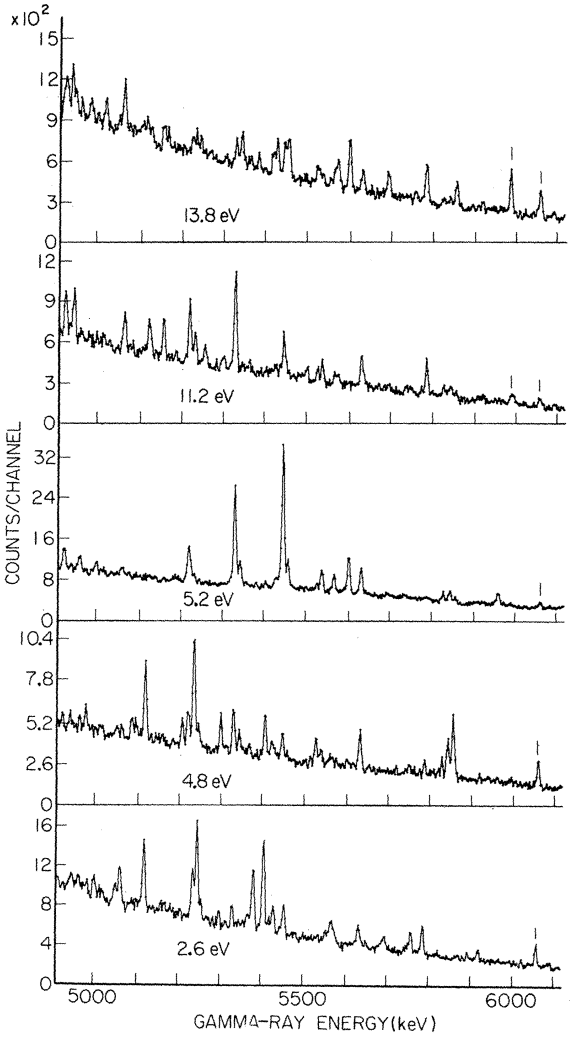

FIG. 2. The γ-ray spectra for individual resonances.

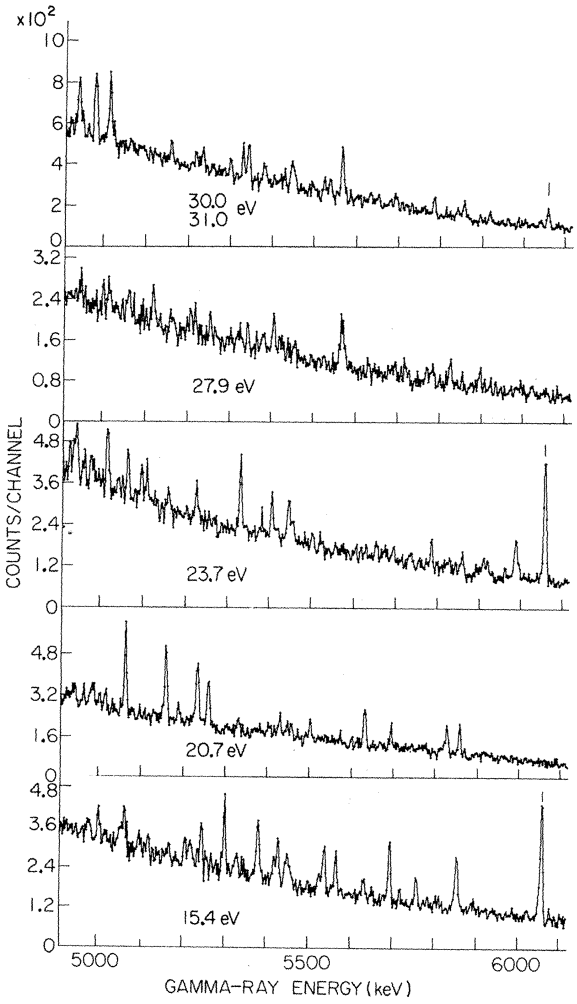

FIG. 3. The γ-ray spectra for individual resonances.

TABLE I. γ-ray energies and intensities from $^{175}Lu(n,\gamma)^{176}Lu$. The γ-ray energies and excitation energies of the populated final states are listed in columns 2 and 3. In order to reduce the size of the table, only the largest energy errors from all entries are listed in parentheses for γ-ray No. 1. Column 4 lists the final-state spin limitations from this experiment. The standard deviations for the γ-ray intensities are listed in parentheses while the underlined intensities are those which exceed twice the standard deviation. For the average intensity, the error is that of the finite statistical sample size, which is larger than the experimental error of 0.3.

Peak No.	E_γ (keV)	E_x (keV)	J_f	I_j (photons per 1000 captures) 2.6 eV	4.8 eV	15.4 eV	27.9 eV
1	6053.8(2.0)	239.4(1.0)	3,4	4.6(0.8)	7.8(1.3)	28.2(3.1)	1.0(1.2)
2	5984.8	308.4	2[a]	0.2(0.6)	1.6(0.8)	1.2(0.8)	0.4(1.2)
3	5856.3	436.9	2[a]				
4	5852.0	441.2	5[a]	−0.4(0.6)	19.6(1.6)	14.6(1.6)	1.2(1.2)
5	5840.6	452.6	3,4	0.1(0.6)	13.0(1.2)	0.5(1.6)	1.0(1.2)
6	5825.1	468.1	3,4	0.6(0.7)	4.3(0.6)	0.5(1.0)	6.6(2.3)
7	5784.2	509.0	3,4	7.6(0.9)	3.7(1.2)	1.4(1.0)	3.5(1.8)
8	5756.6	536.6	(5)	2.4(0.8)	0.8(1.2)	6.2(0.9)	−0.4(1.2)
9	5693.3	599.9	3,4	3.0(0.8)	−0.2(1.0)	13.5(1.5)	2.4(1.4)
10	5631.2	662.0	3,4	6.6(1.0)	12.4(1.2)	5.1(1.4)	2.7(1.6)
11	5601.4	691.8	3,4	6.2(1.0)	2.8(1.2)	0.1(1.0)	−0.4(1.1)
12	5574.3	718.8	3,4	2.0(1.0)	0.5(1.0)	1.0(1.0)	6.0(2.0)
13	5566.6	726.6	3,4	9.5(1.3)	6.4(1.9)	8.8(1.5)	17.6(3.7)
14	5537.3	755.9	3,4	1.8(1.0)	4.5(1.6)	10.8(1.3)	−0.4(1.0)
15	5525.7	767.5	3,4	0.0(1.0)	8.4(2.0)	4.2(0.8)	1.5(1.0)
16	5500.8	792.4	(2)	0.3(1.0)	0.3(1.0)	0.6(0.8)	0.4(1.0)
17	5456.2	837.0	3,4	7.9(1.4)	1.2(1.0)	4.3(1.8)	3.0(1.2)
18	5446.1	847.1	3,4	1.8(1.2)	8.5(1.0)	8.1(1.8)	0.4(1.0)
19	5429.3	864.0	3,4	7.3(1.2)	2.8(1.2)	9.2(1.0)	−0.5(1.0)
20	5420.2	873.0	3,4	2.5(1.2)	4.9(1.3)	5.1(0.8)	1.2(1.2)
21	5405.7	887.5	3,4	24.0(1.8)	13.6(0.8)	0.3(1.0)	5.6(1.2)
22	5382.1	911.1	(5)	1.7(1.2)	−0.3(1.0)	14.8(1.0)	3.0(1.2)
23	5367.8	925.4	(5)	3.5(0.9)	3.4(1.2)	0.4(1.0)	0.8(1.2)
24	5344.6	948.6	3,4	0.1(0.8)	7.1(1.1)	2.1(1.0)	3.8(1.2)
25	5331.5	961.5	3,4	3.6(1.3)	15.5(1.0)	5.2(1.3)	0.9(1.2)
26	5301.2	992.0	(5)	2.8(0.9)	10.1(1.2)	13.2(2.8)	1.1(1.2)
27	5258.7	1034.5	3,4	3.6(1.0)	0.6(1.2)	1.1(1.0)	2.2(1.3)
28	5247.1	1046.1	(5)	22.9(1.1)	6.7(0.8)	7.7(3.5)	6.0(1.4)
29	5235.7	1057.5	3,4	11.9(1.0)	36.4(1.6)	1.7(1.0)	−0.4(1.2)
30	5222.6	1070.6	3,4	−0.2(1.0)	12.0(1.0)	4.5(1.0)	5.4(1.4)
31	5209.8	1083.4	(5)	0.2(1.0)	7.8(0.8)	4.4(1.0)	5.2(1.4)
32	5190.8	1102.4	(2)	−0.2(1.0)	1.2(1.2)	−0.6(1.0)	1.0(1.4)
33	5185.5	1107.7	(2)	0.6(1.0)	2.0(1.2)	−1.0(1.0)	−0.2(1.2)
34	5160.0	1133.2	(2)	1.3(1.0)	1.3(1.1)	1.0(1.0)	2.9(1.5)
35	5121.1	1172.1	3,4	16.3(1.0)	21.1(1.4)	5.0(1.4)	10.2(2.0)
36	5064.4	1228.8	3,4	10.0(1.0)	3.2(1.4)	7.2(1.4)	5.1(2.0)
37	5052.8	1240.4	3,4	5.1(1.0)	4.2(1.4)	4.0(1.5)	0.4(1.5)

[a] Final state spins from Ref. 22.

TABLE I *(Continued)*

I_j (photons per 1000 captures)									
5.2 eV	11.2 eV	13.8 eV	20.7 eV	23.7 eV	36.5 eV	40.6 eV	30.0 31.0 eV	49.5 50.2 eV	$\langle I_j \rangle_{15}$
4.3(0.9)	3.9(0.8)	6.5(1.0)	−0.3(0.6)	27.5(2.0)	0.1(0.8)	9.6(1.5)	4.9(0.5)	16.3(1.6)	9.0(3.0)
0.2(0.5)	3.2(1.1)	9.2(0.8)	0.2(0.6)	12.1(1.5)	3.5(1.0)	1.5(0.8)	0.5(0.6)	12.7(1.2)	4.0(1.3)
2.5(1.3)	2.5(1.3)	5.5(0.7)	9.7(1.5)	4.8(0.8)	7.6(0.7)	0.4(0.8)	3.9(0.8)	0.8(1.0)	2.2(0.8)
								0.8(1.0)	2.5(0.8)
<3.0	4.5(2.0)	1.3(0.8)	1.0(1.0)	1.8(1.0)	4.5(0.7)	<1.5	1.9(0.7)	1.1(1.0)	2.0(0.7)
3.5(1.0)	4.7(1.0)	1.0(0.8)	12.0(3.0)	1.5(1.2)	9.0(0.8)	2.2(0.7)	−0.1(0.7)	−0.3(1.0)	3.1(1.1)
0.4(1.0)	10.6(1.0)	9.1(1.0)	−0.3(1.0)	5.1(1.0)	3.8(0.5)	1.2(0.8)	3.7(0.7)	0.4(1.0)	3.6(1.2)
−0.1(1.0)	0.1(1.0)	1.4(0.8)	−0.4(1.0)	1.5(1.2)	−0.2(0.8)	0.3(0.8)	0.8(0.7)	1.8(0.9)	1.1(0.4)
0.4(1.0)	1.7(0.9)	6.4(0.9)	6.0(1.8)	2.1(1.2)	2.7(1.0)	0.6(0.8)	2.9(1.0)	4.7(0.6)	3.7(1.3)
14.6(1.2)	12.0(1.6)	5.1(0.8)	13.8(1.8)	2.2(1.1)	1.0(1.0)	2.0(0.9)	2.0(0.9)	9.6(1.5)	6.7(2.3)
19.4(2.2)	0.2(0.8)	10.8(1.0)	3.0(0.6)	1.6(1.4)	10.5(1.8)	0.0(0.8)	0.9(0.8)	3.4(1.3)	4.2(1.4)
0.2(1.2)	2.7(0.8)	5.5(1.0)	0.4(1.2)	1.0(1.1)	−0.6(1.1)	<3.0	0.8(0.9)	1.5(1.5)	1.7(0.6)
8.8(1.2)	3.0(0.8)	3.4(0.8)	−0.3(1.2)	0.2(1.1)	−0.2(1.1)	21.7(2.1)	13.1(1.8)	9.0(1.0)	8.2(2.7)
10.3(1.2)	5.5(0.8)	2.2(0.8)	0.2(1.2)	0.8(1.4)	1.8(1.1)	0.2(1.0)	4.5(1.0)	18.5(1.7)	5.6(2.1)
2.7(1.0)	3.6(0.8)	4.5(0.9)	−0.2(1.2)	2.5(1.4)	0.7(1.1)	5.5(0.9)	5.2(1.0)	1.8(2.0)	3.2(1.1)
0.1(1.0)	2.6(1.0)	−0.3(0.9)	5.2(0.7)	4.3(1.4)	−0.2(1.1)	0.0(0.9)	0.5(1.0)	11.0(1.0)	2.4(0.9)
15.3(2.4)	<1.5	9.0(0.9)	3.6(0.7)	4.6(0.8)	3.4(1.1)	8.5(1.3)	3.2(1.4)	5.4(1.0)	5.2(1.7)
76.4(4.6)	12.8(2.7)	7.8(0.8)	3.8(0.7)	9.5(1.0)	17.8(1.9)	22.9(2.0)	5.9(1.5)	4.6(1.0)	12.7(4.3)
7.6(1.9)	2.0(0.9)	8.0(1.2)	6.4(2.0)	0.4(1.0)	3.6(1.1)	0.4(1.2)	1.8(1.0)	0.3(1.0)	3.4(1.2)
0.4(1.0)	0.8(0.8)	4.0(1.2)	1.6(2.0)	2.5(1.0)	0.9(1.1)	5.6(0.7)	1.0(1.0)	11.9(1.5)	3.7(1.3)
2.4(1.0)	1.1(0.8)	−0.2(1.0)	2.9(2.0)	9.0(1.0)	−0.3(1.1)	8.7(0.7)	1.7(1.0)	−0.3(1.0)	5.6(1.9)
1.8(0.9)	0.0(0.8)	2.0(0.8)	1.2(1.2)	2.4(1.2)	0.3(1.1)	0.2(0.9)	4.3(0.8)	0.1(0.9)	2.5(0.9)
0.3(0.9)	4.0(2.3)	1.6(0.8)	1.0(1.2)	0.9(1.2)	−0.3(1.1)	0.4(0.9)	−0.3(0.8)	0.3(0.9)	1.1(0.4)
13.4(1.7)	1.2(0.8)	6.6(0.6)	−1.0(1.2)	2.4(1.2)	20.7(2.3)	3.0(1.0)	7.6(1.0)	1.8(0.9)	5.2(1.8)
51.8(3.4)	32.1(2.8)	4.9(0.6)	3.8(2.3)	13.9(1.2)	6.2(1.3)	24.0(2.5)	6.0(1.0)	15.8(1.5)	14.8(4.9)
0.1(0.9)	1.7(0.9)	0.2(0.8)	−0.3(1.2)	0.5(1.2)	0.4(1.1)	0.6(1.0)	3.2(0.6)	−0.6(0.9)	2.5(0.9)
−0.1(0.9)	7.3(0.8)	0.0(0.8)	17.2(2.1)	1.0(1.2)	4.0(1.2)	1.2(1.0)	1.5(0.8)	0.7(0.9)	2.8(1.0)
1.1(0.9)	0.2(0.8)	2.5(0.8)	1.0(1.2)	0.7(1.2)	0.5(1.2)	1.2(1.0)	0.2(0.8)	1.8(0.9)	5.2(1.8)
4.1(0.9)	9.8(1.0)	2.8(0.8)	25.6(3.1)	1.2(1.2)	4.0(1.6)	7.0(3.2)	4.6(1.7)	9.4(1.5)	8.8(3.2)
21.5(1.7)	18.7(1.2)	3.4(0.8)	1.8(1.2)	5.1(1.3)	2.4(1.1)	1.0(1.0)	3.1(1.0)	−0.1(1.0)	5.4(1.9)
−0.3(0.9)	−0.6(1.0)	−0.2(0.8)	1.0(1.2)	0.5(1.2)	0.6(1.1)	−0.5(1.0)	0.7(0.8)	3.0(1.0)	1.7(0.6)
0.8(0.9)	2.2(1.0)	0.2(0.8)	2.6(1.2)	−0.8(1.2)	8.2(2.4)	−0.2(1.0)	0.3(0.8)	7.5(1.7)	2.0(0.7)
0.7(0.9)	0.3(1.0)	0.2(0.8)	3.1(1.2)	0.1(1.2)	4.1(2.0)	1.2(1.0)	−0.5(0.8)	1.2(1.0)	1.0(0.4)
0.8(0.9)	10.4(1.8)	5.5(1.8)	25.6(2.7)	4.1(1.2)	3.8(1.3)	5.1(1.1)	4.3(1.0)	−0.5(1.0)	4.7(1.7)
0.1(0.9)	9.9(1.0)	4.6(1.2)	−0.6(1.2)	4.3(1.0)	0.3(1.2)	−0.1(1.0)	1.2(0.8)	7.8(1.2)	5.9(2.1)
3.0(1.0)	3.1(1.0)	5.8(1.3)	24.5(2.2)	8.2(1.4)	3.8(1.3)	4.3(1.1)	2.2(0.9)	3.6(1.2)	6.0(2.2)
1.0(1.0)	1.4(1.0)	3.5(1.3)	1.8(1.4)	1.8(1.4)	2.4(1.3)	8.4(1.2)	0.1(0.9)	0.2(1.2)	2.3(0.8)

in each γ-ray spectrum for energies exceeding 4.0 MeV is a measure of the number of neutrons captured. This is reasonable because of the large number of γ rays observed. The ratio of the γ-ray peak area to the total counts in each spectrum then gives the relative γ-ray intensity. The absolute γ-ray intensities in units of photons per 1000 captures are obtained by normalization to previously measured thermal-capture intensities. The intensity standard selected is 8.3 photons per 1000 captures in ^{175}Lu measured for the 5984.7-keV γ ray in thermal capture by Minor *et al.*[22] Since the resonance spectra were measured with a natural sample whose thermal-capture spectrum contains an approximately 80% contribution from the ^{176}Lu impurity, a sample enriched to 99.93% ^{175}Lu was used for the thermal-capture measurement. The contribution of the ^{176}Lu impurity to this thermal spectrum, which was calculated to be about 2%, was ignored. The individual γ-ray peak areas were determined from a nonlinear least-squares fitting of a Gaussian peak shape with a linear background. The observed peak areas are also corrected for the variation of detector efficiency with γ-ray energy. The efficiency was deduced from the nitrogen thermal-capture γ rays emitted in a melamine sample using the γ-ray intensities of Rasmussen *et al.*[29] as a standard. The resulting γ-ray intensities are listed in Table I. The errors result from the uncertainty in the peak areas.

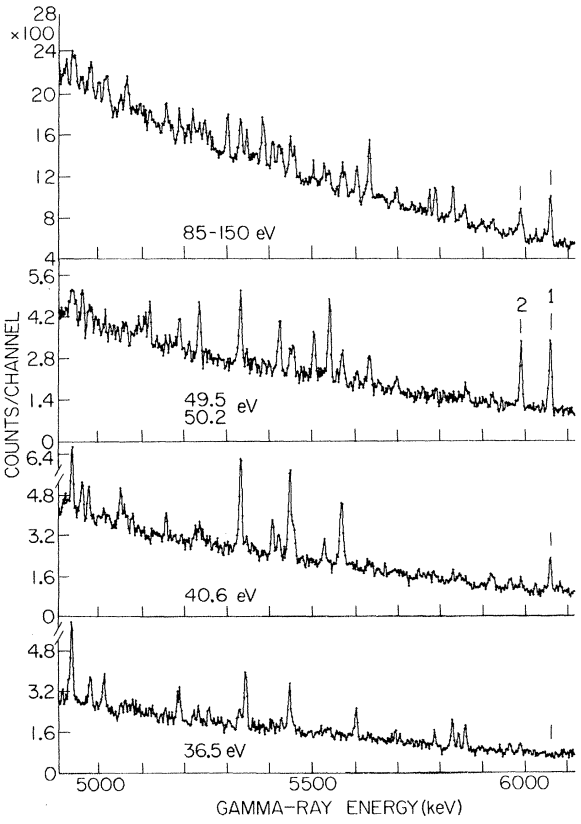

FIG. 4. The γ-ray spectra for individual resonances.

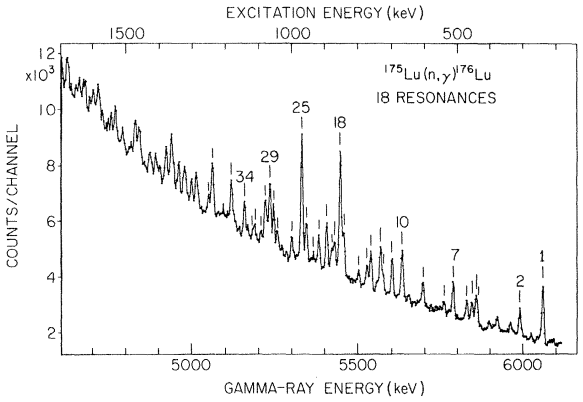

FIG. 5. The γ-ray spectrum for the sum of 18 resonances.

C. Average γ-Ray Intensities

The intensity of the γ rays averaged over 15 resonances is shown in Fig. 6. The error bars indicate the error in the mean ($\pm\sqrt{\frac{\chi}{15}}$) due to the limited statistical sample of 15 cases, assuming the individual γ rays to have a χ^2 distribution with one degree of freedom. The statistical error exceeds that due to the uncertainty in the γ-ray peak areas except for the weak γ rays, where both sources of error are comparable. There is no obvious arranging of the γ rays into groups which can be associated with the final-state spins, as has been done for some nuclei.[30] There is also no obvious grouping which depends on the γ-ray multipolarity, although it is suggested that the weaker lines may be magnetic dipole, which would require positive parity for those final states. The different symbols indicating spin assignments used in Fig. 6 are

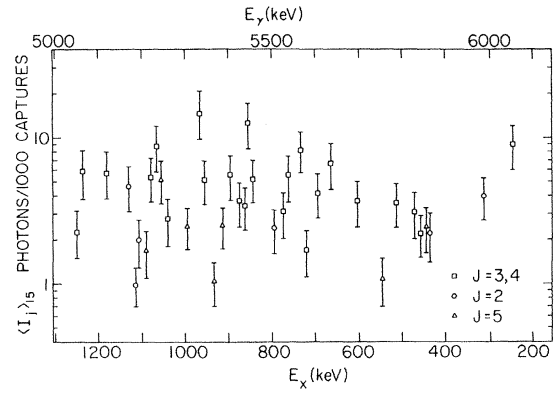

FIG. 6. The γ-ray intensities averaged over 15 resonances.

those which are favored by this experiment and listed in Table. I.

IV. DETERMINATION OF RESONANCE SPINS

A. High-Energy γ Rays

In order to determine the spins of the 11 resolved resonances, both the high- and low-energy γ-ray spectra from individual resonances are used. We have previously shown that no final-state spin information is obtained from the combined high-energy spectrum. The target nucleus ^{175}Lu has spin and parity $\frac{7}{2}^+$. For s-wave neutron capture the resulting resonance spin and parity are 3^+ or 4^+. We

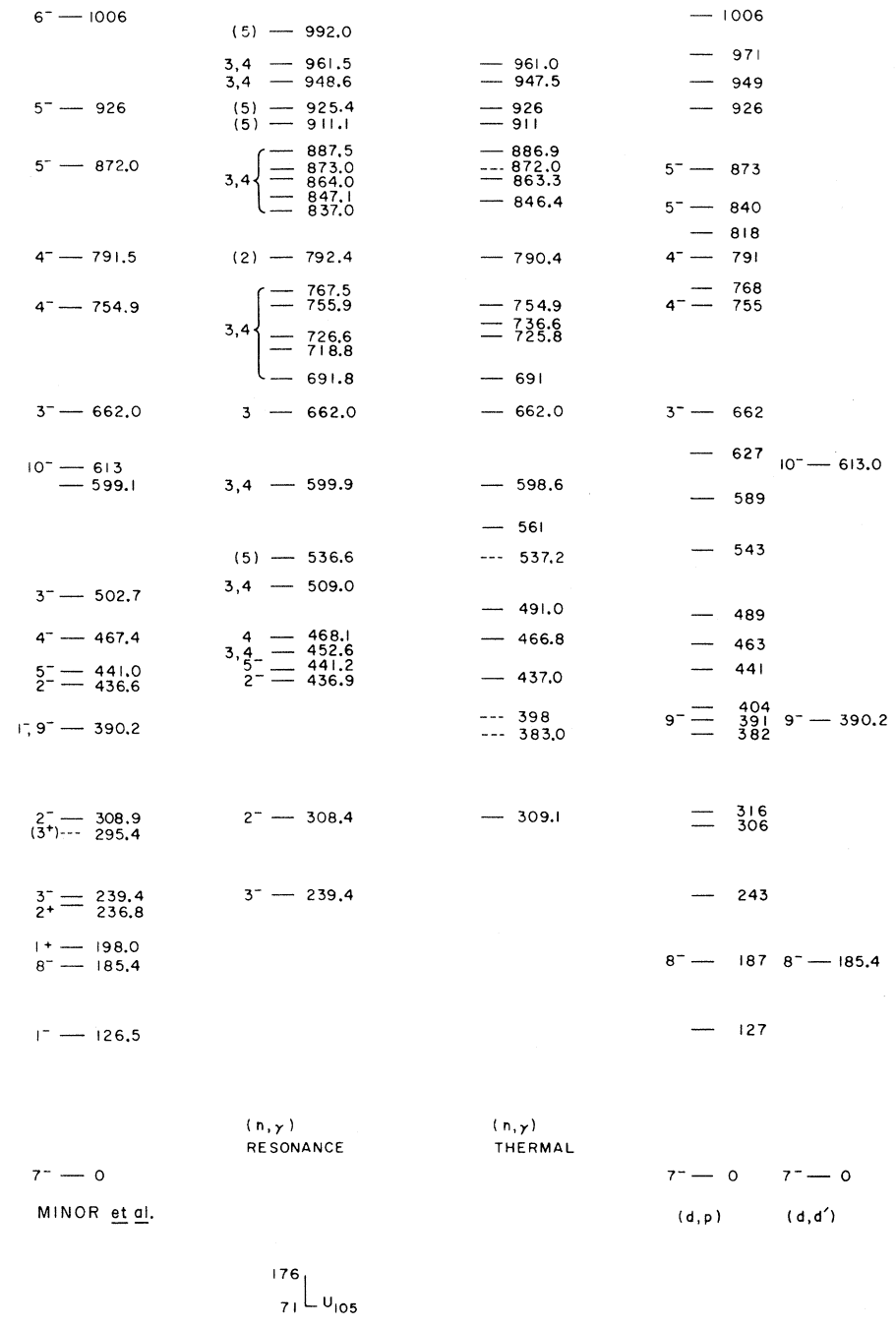

FIG. 7. The energy-level diagram of ^{176}Lu. The levels from the recent work of Meiner *et al.* are shown on the left, while the present resonant (n,γ) results are shown along with those from other reactions.

assume only dipole transitions to be observable, so that final states of spin 2 can only be populated by primary transitions from the spin-3 resonances, while spin-5 final states are populated only from the spin-4 resonances. This criterion for deducing the resonance spins requires a knowledge of the final-state spins.

The energy-level diagram deduced by Minor *et al.*[22] is shown in Fig. 7. This level scheme uses the excitation energies deduced from thermal-neutron-capture γ rays and internal-conversion electrons, the (d,p) reaction, elastic deuteron scattering, as well as γ-γ coincidences between the low-energy γ rays. Note that 2^- states are observed at 308.9 and 436.6 keV, while a 5^- state is located at 441.0 keV. However, these final states are populated strongly in only 6 of the 11 resonances. Also the 2^- and 5^- states at 436.6 and 441.0 keV are separated by only 4.4 keV. Since only one of these two states may be populated in a given resonance, a careful determination of this γ-ray peak position is done for each resonance, taking into account the contribution of a nearby single-escape peak. The locations of the peaks are shown in Fig. 8. In only five resonances are the peaks strong enough to establish a peak position of sufficient accuracy to produce definite resonant spin assignments. These five resonances are indicated by open and closed circles in the spectrum. The point at 30 eV, which includes two unresolved resonances, demonstrates that at least one of the resonances has spin 3. An additional spin assignment follows from consideration of the γ-ray transition to the other 2^- state at 308.9 keV, which yields spin 3 for the 11.2-eV resonance. In this manner 6 of the 11 resonance spins are assigned. For the remaining 5 resonances use is made of the low-energy γ-ray spectra.

B. Low-Energy γ Rays

From very simple assumptions the relative populations of the low-lying states through multiple γ-ray cascades is expected to depend upon the spins of the capturing state as well as the final state. Following the work of Draper, Fenstermacher, and Schultz,[31] who observed the variation in the intensities of the low-energy γ rays for various resonances, several authors[32-37] have subsequently used this simple model to deduce the resonance-state spins for different nuclei. This simple model assumes that the population of a final state depends on the total number of ways it can be reached in various cascades from the capturing state. It has been observed in several experiments that systematic differences in the low-energy spectra do exist, and that these differences can be related to the spin of the capturing state. This method is applied to the lutetium.

The low-energy ($E_\gamma < 800$ keV) γ-ray spectra were obtained with the isotopically enriched sample at the 48-m flight path using a 37-cc Ge(Li) detector. Two examples of spectra showing only the useful γ-ray energy interval are shown in Fig. 9. The three γ rays used to assign resonance spins are indicated. These are relatively intense transitions, which are resolved from nearby γ rays and are located in the decay scheme by Minor *et al.*[22] The γ-ray energy as well as the spin of the emitting state are shown above the three peaks. The remaining strong γ-ray peaks either contain several γ rays or are not located in the decay scheme. It is observed that the intensity of the γ ray from the 5^- state relative to that from the 1^- state is larger in the 4.8-eV resonance. Using the peak-fitting program to measure the γ-ray peak areas in each spectrum results in the ratios of peak areas shown in Fig. 10. The spins and excitation energies of the three emitting states, as assigned by Minor *et al.*,[22] are indicated in the figure. The ratios of γ-ray intensities clearly fall into two groups, which are indicated by circles and triangles. The points indicated by squares result from unresolved resonances and are ignored. The same grouping into 7 and 4 members is observed for both ratios. The horizontal lines represent the mean values for each group. The two groups are identified with the two possible values of the resonance spins. Which group to associate with a given resonance spin is determined from the previous assignments from the high-energy γ-ray spectra. In this manner the spins are assigned to the 11 resonances, as is indicated in Table II. In every case the high-energy spin assignments are consistent with the low-energy grouping. The separation of the low-energy spectra into two groups in lutetium is regarded as an empirical fact, which is not dependent upon the particular location of the low-en-

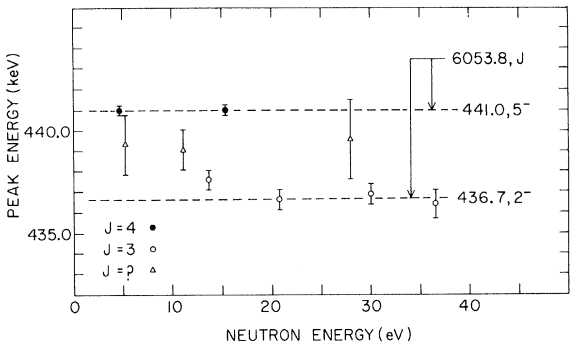

FIG. 8. Determination of resonance spins from the peak position of the primary γ-rays populating either the 2^- or 5^- state. The γ-rays indicated by triangles are too weak to determine which state is populated.

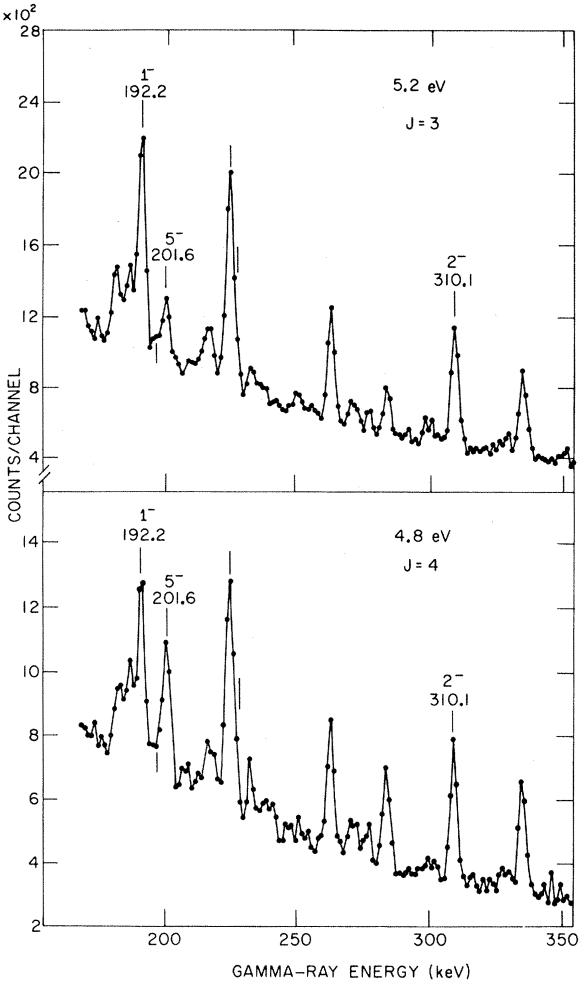

FIG. 9. Example of low-energy γ-ray spectra. The three γ rays used to determine resonance spins are labeled by the γ-ray energy, spin, and parity of emitting state.

ergy γ rays in the decay scheme. Thus the resonance spin assignments will be unaffected by any subsequent revisions in the placement of these low-energy γ rays in the decay scheme.

V. LIMITATION OF FINAL-STATE SPINS

Having established the resonance spins it is now possible to use the results of the measured high-energy γ- ray intensities to limit the spin values of the final states. The reasonable assumption is made that only $E1$ or $M1$ transitions from the capturing states are intense enough to be observed. It is further assumed that all the γ rays above 5000 keV in energy are primary transitions from this capturing state. With these reasonable assumptions, all 37 γ rays listed in Table I populate final states with spins 2, 3, 4, or 5. The observation of a γ ray in both a spin-3 and spin-4 resonance

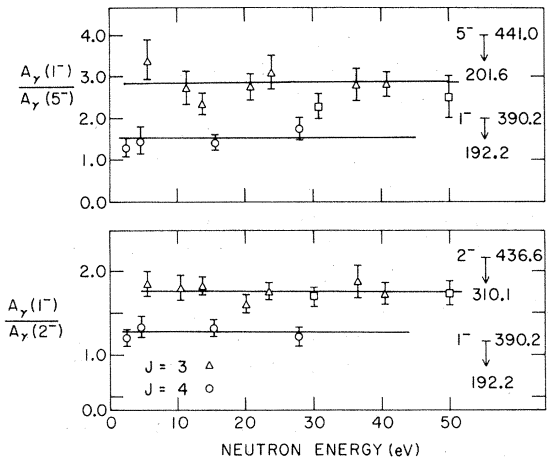

FIG. 10. Ratios of γ-ray peak areas from various resonances used in the determination of resonance spins. The rectangular symbols result from unresolved resonances. The horizontal lines indicate the mean values for each spin group.

further limits the final-state spin to a value of 3 or 4. The criterion used to select "observable" γ rays is that the intensity exceed twice the standard deviation. The γ rays which meet this requirement are underlined in the table. In this way 24 of the 37 γ rays are limited to final states of spins 3 or 4, as is shown in the fourth column in Table I.

The determination of final states of spin 2 and 5 is less certain because of the large variation in γ-ray transition probabilities from resonance to resonance. For these cases statistical arguments are used, and for that reason the proposed final states of spin 2 or 5 are enclosed in parentheses in Table

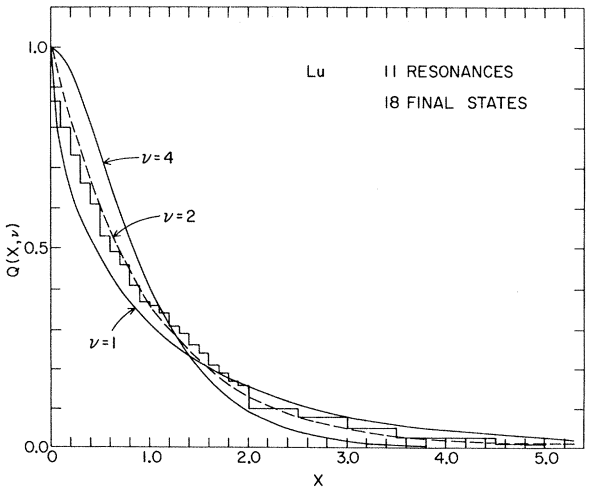

FIG. 11. Distribution of 198 γ-ray intensities in lutetium. The horizontal axis is the individual intensity relative to its mean value over resonances. The histogram is the experimental data, while the curves are calculated for different degrees of freedom.

I. For calculational purposes it is assumed that each γ-ray intensity is distributed over resonances according to a χ^2 distribution with one degree of freedom. For this distribution there is a 50% probability for the γ-ray intensity to be less than one half the mean value. For the weaker γ rays, the experimental sensitivity is approximately one half the mean intensity, which indicates that the probability of not observing a γ ray in m resonances is equal to $(\frac{1}{2})^m$. This yields a 6.7 and 1.7% probability of not observing a certain γ ray in a total of 4 and 7 resonances, respectively. Using these results, there is an approximately 93% probability that the failure to observe a particular γ ray in any of the four spin-4 resonances occurs because the final-state spin is 2. Correspondingly, there is an approximately 98% probability that the final-state spin is 5 if the γ ray is not observed in any of the seven spin-3 resonances. This statistical argument is the evidence for the six spin-2 and seven spin-5 assignments in Table I. Let us next compare these spin assignments with the previous results of Minor *et al.*[22]

VI. DISCUSSION OF THE LEVEL SCHEME

The low-lying energy levels observed in the present resonant (n,γ) experiment are shown in Fig. 7 along with those deduced from previous experiments. A comparison of the results of the present experiment with those of Minor *et al.*[22] indicates a few differences. The comparison is restricted to the final-state spins of 2, 3, 4, or 5 which can be populated in the (n,γ) experiment. The positive-parity states at 236.8 and 295.4 keV are not observed in the present experiment, which indicates that either the required $M1$ γ-ray intensities to these states are too weak to be observed or the spin assignments are incorrect. The experiment can not determine which alternative applies. The proposed 3^- state at 502.7 keV is not populated in the resonant (n,γ) reaction. Since the probability of observing at least one $E1$ transition to this state in 11 resonances is greater than 99.9%, the location of this state is questioned.

However, these inconsistencies are sufficient to require a revision of the location of a few rotational bands. Minor *et al.*[22] have placed six rotational bands based on the coupling of the 71st proton in the $\frac{7}{2}^+[404]$ Nilsson orbital to the 105th neutron in the $\frac{7}{2}^-[514]$, $\frac{9}{2}^+[624]$, $\frac{5}{2}^-[512]$, and $\frac{1}{2}^-[510]$ orbitals. The parallel and antiparallel coupling of each proton and neutron orbit produces two rotational bands. Six of the eight possible bands are placed in the level diagram. Of these six bands four couplings lead to negative-parity final states with spins which are accessible to $E1$ γ-ray decay from the capturing states. These four bands are the $0^-[404^\downarrow - 514^\downarrow]$, $1^-[440^\downarrow - 512^\uparrow]$, $3^-[404^\downarrow - 510^\uparrow]$, and $4^-[404^\downarrow + 510^\uparrow]$.

The present experiment is consistent with the states assigned to the $0^-[404^\downarrow - 514^\downarrow]$ rotational band.

The failure to observe the proposed 3^- state at 502.6 keV in the present experiment calls for a revision of the states assigned to the $1^-[404^\downarrow - 512^\uparrow]$ band. Assuming the band head to be properly located, we propose the previously unobserved state at 509.0 keV as the 3^- member of the band. Using the one-parameter rotational formula

$$E(I) = E_0 + AI(I+1)$$

and the energies of the 1^- and 2^- members of the band, we obtain

$$A = 11.6 \text{ keV}.$$

This value of the parameter then predicts the 3^- and 4^- members to lie at 506.2 and 599.0 keV, respectively. It is thus suggestive that the levels at 509.0 and 599.8 keV are the 3^- and 4^- members of this rotational band. The 5^- member is then predicted to be at 716 keV, but there is no state of possible spin 5 near that energy. Ignoring the 5^- state, the resonant (n,γ) results are consistent with the previously assigned location of the band head of the $1^-[404^\downarrow - 512^\uparrow]$ rotational band, but require a different identification of two of the individual band members.

For the $3^-[404^\downarrow - 510^\uparrow]$ band the present experiment requires that the previously proposed 5^- member at 872 keV actually has a spin of 3 or 4. This observation questions the placement of this rotational band. Similar doubt is raised concerning the location of the $4^-[404^\uparrow - 510^\uparrow]$ band. The present experiment strongly suggests that the pro-

TABLE II. Resonance spin assignments.

Resonance energy (eV)	Resonance spin High-energy γ rays	Low-energy γ rays
2.6		4
4.8	4	4
5.2		3
11.2		3
13.8	3	3
15.4	4	4
20.7	3	3
23.7	3	3
27.9		4
36.5	3	3
40.6		3

posed band head is not at 791.5 keV, as was previously proposed, since the spin of that state is probably equal to 2. There are not sufficient data to determine the proper location of these bands.

In addition, the low-lying levels at 452.6 and 536.6 keV are unassigned to various bands. These considerations demonstrate that the nuclear configurations of the low-lying states in ^{176}Lu are not completely known and that much further work is required before final assignments are determined.

VII. DISTRIBUTION OF PARTIAL RADIATION WIDTHS

For a nucleus which has the statistical properties assumed by Porter and Thomas,[1] the variation over capturing states of the partial radiation widths is predicted to follow a χ^2 distribution with one degree of freedom. To test for the validity of the statistical hypothesis in ^{175}Lu(n,γ), it is assumed that the distribution of experimental widths is describable by the general class of χ^2 distribution functions with ν degrees of freedom. The method of analysis is to find the value of the parameter ν which best fits the data, allowing ν to assume nonintegral values.

The experimental quantities measured in the experiment are the γ-ray intensities $I_{\lambda j}$, which for isolated resonances are given by

$$I_{\lambda j} = 1000(\Gamma_{\lambda j}/\Gamma_{\lambda}),$$

where $\Gamma_{\lambda j}$ is the partial radiation width for a γ-ray decay from resonance λ to final state j, and Γ_{λ} is the total radiation width for resonance λ. Since there is no contrary evidence, it is assumed that the total radiation widths are constant, so that the partial radiation widths are proportional to the γ-ray intensities. This means that λ-ray intensities may be used to determine the distribution of partial radiation widths.

The integral distribution of the 198 γ-ray intensities for 11 resonances and 18 final states are shown by the histogram in Fig. 11. The horizontal scale contains the quantity $X_{\lambda j}$ given by

$$X_{\lambda j} = I_{\lambda j}/\langle I_{\lambda j}\rangle_{\lambda},$$

where $\langle I_{\lambda j}\rangle_{\lambda}$ is the average over the 11 resonances of the γ-ray intensity populating final state j. Only those final states of spin 3 or 4 which could be populated by dipole transitions from resonances of both spins are included in the analysis. The curves represent the integral χ^2 distributions with 1, 2, and 4 degrees of freedom. The histogram, which lies between the curves for $\nu=1$ and $\nu=2$, clearly is nearer the $\nu=2$ curve.

In order to determine the number of degrees of freedom which best fits the experimental data, a program described fully in a previous publication[6] is used. A Monte Carlo program generates partial widths from χ^2 distributions with various degrees of freedom. Normally distributed experimental errors are then added to these widths. The mathematical and physical samples are analyzed in the same manner by both the method of maximum likelihood (ML) and relative variance (RV). The results are

$$\nu(\mathrm{RV}) = 1.62^{+0.42}_{-0.30}$$

and

$$\nu(\mathrm{ML}) = 1.56^{+0.30}_{-0.23},$$

where the limits represent the 10 and 90% values of the integral distribution. The two methods of analysis yield comparable results. In both cases the probability that $\nu \leq 1$ is less than 1%, while there is a 6 and 15% probability that ν exceeds 2 for the ML and RV analyses, respectively. It is concluded that the distribution of partial radiation widths in lutetium is inconsistent with a χ^2 distribution with one degree of freedom.

In order to further investigate the distribution of partial widths, many different subgroups of γ-ray intensities were analyzed. The intensities were grouped into classes according to the resonance spin and further divided depending on average γ-ray intensity as well as specific properties of the final states. The results are shown in Table III. In all cases the distribution of the number of degrees of freedom has at least a 10% probability of including the value of 1.62 observed for the larger set, although the value is different in some cases for the different resonance spins.

The examples in Table III suggest that the number of degrees of freedom of the various subsets of γ rays differ. However, the statistical errors

TABLE III. Distributions of γ-ray intensities for various combinations fo γ rays grouped according to resonance spin.

γ-ray subgroups	ν(RV) $J=3$	$J=4$
7 γ rays for $E_x < 660$ keV	$2.02^{+1.0}_{-0.64}$	$0.98^{+0.60}_{-0.44}$
7 Strongest γ rays	$1.38^{+0.50}_{-0.42}$	$2.75^{+1.8}_{-1.2}$
13 γ rays for $E_x < 660$ keV	$1.35^{+0.60}_{-0.25}$	$1.88^{+0.82}_{-0.38}$
13 γ rays to states with small (d,p) cross sections	$1.55^{+0.45}_{-0.38}$	$1.35^{+0.55}_{-0.40}$
5 γ rays to states with large (d,p) cross sections	$2.0^{+1.3}_{-0.75}$	$2.35^{+1.5}_{-1.1}$
18 γ rays	$1.64^{+0.40}_{-3.0}$	$1.54^{+0.45}_{-0.34}$

are too large to justify a firm conclusion. Reducing the statistical error must await future experiments which can resolve many more resonances. The conclusion from the analysis of various subsets of γ rays is that the departure from one degree of freedom is not limited to any particular group of γ rays.

A possible source of the observation of more than one degree of freedom is correlations among γ-ray intensities. If such correlations occur, the effective size of the statistical sample is reduced resulting in an underestimate of the statistical error. However, it is later shown that no such correlations occur, and this source of error is eliminated from consideration. Removing the five most-correlated γ rays from the analysis yields $\nu = 1.82^{+0.43}_{-0.34}$, which is consistent with the result for the total group.

The fact that there may be $M1$ as well as $E1$ transitions will not distort the distribution, since each γ-ray intensity is measured relative to its own mean value over resonances. Only large $M1$-$E2$ admixtures in the intensities to final states of positive parity could increase the observed number of degrees of freedom, and this possibility is unlikely.

The final conclusion is that the number of degrees of freedom for the distribution of partial radiation widths is larger than the value of unity predicted by Porter and Thomas[1] but is less than two.

VIII. CORRELATION ANALYSIS

Various reaction mechanisms predict correlations between partial radiation widths and reduced neutron widths of capturing and final states. As a measure of the correlations, use is made of the correlation coefficient T defined by

$$T(\gamma_i,\gamma_j)=\Big[\sum_{\lambda=1}^{n}(I_{\lambda i}-\langle I_{\lambda i}\rangle_\lambda)(I_{\lambda j}-\langle I_{\lambda j}\rangle_\lambda)\Big]/n\sigma_{\lambda i}\sigma_{\lambda j}; \quad (1)$$

where

$$\sigma_{\lambda i}{}^2=n^{-1}\sum_{\lambda}(I_{\lambda i}-\langle I_{\lambda i}\rangle_\lambda)^2$$

is the variance of the distribution, $I_{\lambda i}$ labels the γ-ray intensity, λ labels the resonances, and i and j label the final states. This definition applies only for correlations between pairs of γ rays. For correlations between reduced neutron widths and γ-ray intensities, the γ-ray intensities $I_{\lambda j}$ are replaced with the reduced neutron widths of the capturing state $\Gamma^0_{\lambda n}$, and the resulting correlation coefficients are labeled with R instead of T.

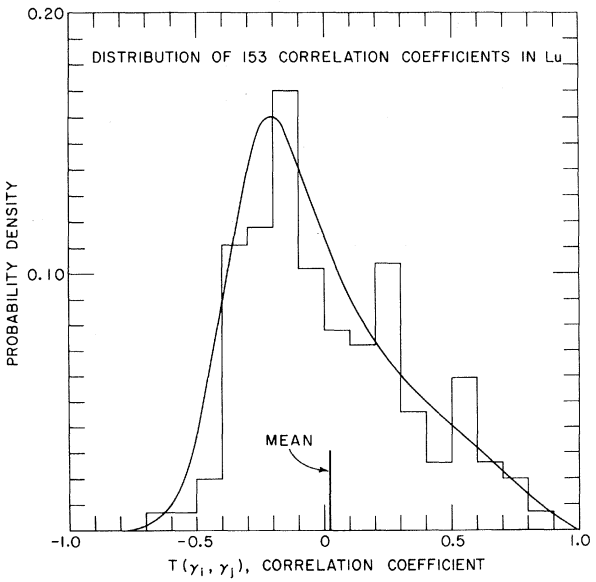

FIG. 12. Differential distribution of correlation coefficients between pairs of γ rays over 11 resonances. The solid curve is that calculated for no correlation.

A. Correlation Between Pairs of γ-Ray Intensities

First let us study the correlations between pairs of γ-ray intensities. If these intensities are not correlated with another quantity, they should be independent of each other. The distribution of the 153 correlation coefficients for the 18 γ-ray intensities to final states of spin 3 and 4 from 11 resonances are shown by the histogram in Fig. 12. The curve is that calculated for zero correlation for 11 resonances. For the calculated curve it is assumed that the γ-ray intensities follow a χ^2 distribution with one degree of freedom. A Monte Carlo program selects uncorrelated samples from the above distribution of widths and calculates the distribution of correlation coefficients for a sample size of 11 quantities. The asymmetrical shape of the null distribution results in the non-normal distribution of γ-ray intensities. The agreement between curve and the histogram demonstrates no correlation among the 18 γ-ray intensities. The mean value of the 153 coefficients is +0.019, which is also consistent with zero correlation.

The largest correlation coefficient, which has a value of +0.87, occurs between the two strongest γ rays, which populate final states at 847.1 and 961.5 keV. These states share no particular common nuclear-structure properties; the 847.1-keV state is part of a doublet strongly populated in the d,p reaction, while the 961.5-keV state is not observed in that reaction. This large coefficient is a demonstration of the statistical variations which can occur in a sample size of 18 γ rays and 11 resonances.

It is interesting to observe the distribution of correlation coefficients from various subsets of γ

rays. The distribution of the 10 correlation coefficients from the 5 most intense γ rays, as well as the 5 γ rays most strongly correlated with the reduced neutron widths of the capturing states, are totally consistent with zero correlation. The mean values of the correlation coefficients of +0.10 and +0.06 have probabilities of 9 and 18%, respectively, of being exceeded for zero correlation. On the other hand, the subset of 7 γ rays to final states strongly populated in the (d,p) reaction shows a small positive correlation. The observed mean correlation coefficient of +0.16 has only a 2% probability of being exceeded for zero correlation. This indicates that these 7 final states share weakly some common nuclear property, which is later shown not to be the magnitude of the (d,p) cross section. This correlation in the subgroup of 7 γ rays is not considered large enough to affect the distribution of the 18 γ-ray intensities.

B. Correlations Between γ-Ray Intensities and Reduced Neutron Widths of Capturing States

The comparison between the reduced neutron widths of the capturing states and the γ-ray intensities is demonstrated in Fig. 13. The reduced neutron widths, determined from the recommended values of $g\Gamma_n^0$ listed in the literature,[38] are shown by the solid bars, while the summed γ-ray intensity to the 8 final states populated strongly in the (d,p) reaction are shown by open bars. There is no correlation. Analysis of the 18 correlation coefficients between the 18 γ rays and the reduced neutron widths also yields a distribution consistent with zero correlation.

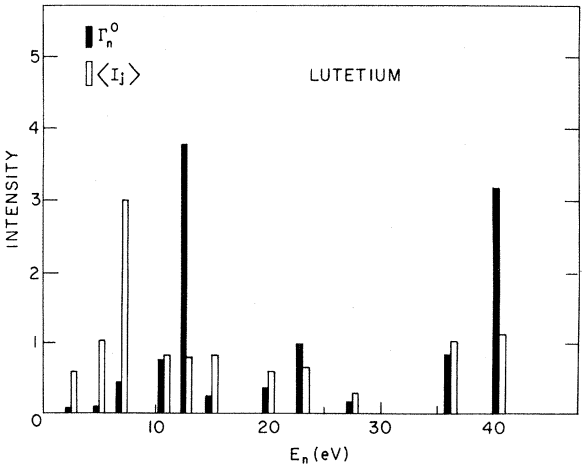

FIG. 13. Comparison of reduced neutron widths of the capturing states with the corresponding average γ-ray intensity for 11 resonances.

C. Correlations Between γ-Ray Intensities and (d, p) Cross Section

Another type of correlation observed for many nuclei is that between the partial radiation widths and the reduced neutron widths of the corresponding final states. Existence of such a correlation in resonance capture is evidence for channel capture,[13] while such correlations in thermal capture are attributed to a direct-capture process. Unfortunately, for lutetium the reduced neutron widths of the final states are unknown. The (d,p) experiments of Struble and Sheline[23] list only the relative intensity of the stronger proton groups at three angles. The value of the orbital angular momentum of the captured neutron as well as the spectroscopic factor are unknown. The interpretation of the correlation analysis is significant only for those final states involving one unit of orbital angular momentum of the capture neutron. However, lacking further evidence, the value of the relative proton intensity at 55° will be used in the analysis.

In this case the definition of the correlation coefficient R in Eq. (1) is changed slightly. The summation and averaging are over final states j instead of capturing states λ. There now results a correlation coefficient for each resonance. The mean value of the 11 correlation coefficients for the 11 resonances is found to be consistent with zero correlation for all combinations of final states tested, which included the following:
(1) the 7 states with the largest (d,p) cross section;
(2) all 18 final states, where $\sigma(d,p)$ is equated to zero for those intensities not listed by Struble and Sheline;
(3) the 10 final states with small (d,p) cross sections.
The lack of correlation is shown in Fig. 14, which

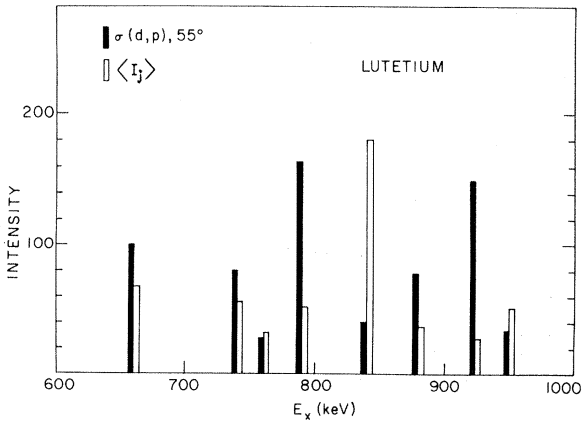

FIG. 14. Comparison of the γ-ray intensity averaged over 11 resonances with the relative (d,p) cross section for 8 final states.

compares the γ-ray intensity averaged over resonances with the relative (d,p) cross sections of the corresponding final states.

The evidence from the analyses of the various correlation coefficients is that there is little correlation between the γ-ray intensities and the reduced neutron widths of either the capturing or final states. Except for the small correlation observed for the 7 γ rays leading to states strongly excited in the (d,p) reaction, there is no significant correlation among individual γ-ray intensities. This lack of correlations demonstrates that the channel-resonance-capture reaction mechanism of Lane and Lynn[13] and the doorway-state contributions are of little importance for excitations above the neutron binding energy in lutetium.

IX. SUMMARY AND CONCLUSIONS

The present investigation of resonant neutron capture yields the spins of 11 neutron resonances in ^{176}Lu from a combination of high- and low-energy capture γ-ray spectra. Additional energy levels were populated which were not observed in previous nuclear-reaction studies. Limitations were placed on the final-state spin values, which were inconsistent with previous assignments in a few cases. These minor discrepancies demonstrate that the nuclear configurations of the low-lying states are still uncertain.

No correlations between the partial radiative widths and reduced neutron widths of either capturing or final states were observed, which indicates that neither the channel-capture process nor doorway-state formation contribute strongly to the capture process. The above evidence indicates that the only departure from the purely statistical compound-nuclear formation in lutetium is the significant inconsistency with the Porter-Thomas distribution of partial radiative widths.

ACKNOWLEDGMENTS

The authors thank Dr. Mendel Beer for interesting discussions and Mrs. Anne Cornelius Jones for her assistance in analyzing the data.

---

†Work performed under the auspices of the U. S. Atomic Energy Commission.

[1]C. E. Porter and R. G. Thomas, Phys. Rev. 104, 483 (1956).

[2]L. M. Bollinger, R. E. Coté, R. T. Carpenter, and J. P. Marion, Phys. Rev. 132, 1640 (1963).

[3]H. E. Jacskon, Phys. Rev. 134, B931 (1964).

[4]C. Samour, H. E. Jackson, J. Julien, A. Block, C. Lopata, and J. Morgenstern, Nucl. Phys. A121, 65 (1968).

[5]O. A. Wasson, R. E. Chrien, M. A. Lone, M. R. Bhat, and M. Beer, Nucl. Phys. A132, 161 (1969).

[6]D. L. Price, R. E. Chrien, O. A. Wasson, M. R. Bhat, M. Beer, M. A. Lone, and R. Graves, Nucl. Phys. A121, 630 (1968).

[7]M. Beer, R. Graves, O. A. Wasson, M. R. Bhat, S. F. Mughabghab, K. Rimawi, D. I. Garber, and R. E. Chrien, Bull. Am. Phys. Soc. 13, 1421 (1968).

[8]M. Beer, Phys. Rev. 181, 1422 (1969).

[9]L. Estrada and H. Feshbach, Ann. Phys. (N.Y.) 23, 123 (1963).

[10]N. Rosenzweig, Phys. Rev. Letters 6, 123 (1963).

[11]T. J. Krieger and C. E. Porter, J. Math. Phys. 4, 1272 (1963).

[12]N. Rosenzweig, J. E. Monahan, and M. L. Mehta, Nucl. Phys. A109, 437 (1968).

[13]A. M. Lane and J. E. Lynn, Nucl. Phys. 17, 563, 586 (1960).

[14]C. K. Bockelman, Nucl. Phys. 13, 205 (1959).

[15]H. Ikegami and G. T. Emery, Phys. Rev. Letters 13, 26 (1964).

[16]A. M. Lane, *Neutron Capture γ-Ray Spectroscopy* (International Atomic Energy Agency, Vienna, Austria, 1969), p. 513.

[17]M. Beer, to be published.

[18]M. Beer, M. A. Lane, R. E. Chrien, O. A. Wasson, M. R. Bhat, and H. R. Meuther, Phys. Rev. Letters 20, 340 (1968).

[19]J. A. Harvey, D. J. Hughes, R. S. Carter, and V. E. Pilcher, Phys. Rev. 99, 10 (1955).

[20]J. A. Harvey, R. Block, and G. G. Slaughter, Bull. Am. Phys. Soc. 3, 364 (1958); Oak Ridge National Laboratory Report No. ORNL 2718, 1959 (unpublished), p. 26.

[21]S. Wynchank, private communication.

[22]M. M. Minor, R. K. Sheline, E. B. Shera, and E. T. Jurney, Phys. Rev. 187, 1516 (1969).

[23]G. L. Struble and R. K. Sheline, Yadern, Fiz. 5, 1205 (1967) [transl.: Soviet J. Nucl. Phys. 5, 862 (1967)].

[24]B. P. K. Maier, Z. Physik 184, 153 (1965).

[25]P. T. Prof'ev, M. K. Balodis, J. J. Berziń, V. A. Bondarenko, M. D. Kramer, Z. J. Lune, G. L. Rozvaya, and L. I. Simonova, *Atlas Spektrov Konversionnykh Elektronov, Ispuskaemykh pri Zabjvate Teplouykh Neitronou Yedrami s A143-197, u Skheny Radiatsionnykh Perekhodov* (Zinatne, Abademiya Navk Letvuskai S.S.R., Riga, U.S.S.R., 1967), p. 75.

[26]R. E. Chrien and M. Reich, Nucl. Instr. Methods 53, 93 (1967).

[27]M. R. Bhat, B. R. Borrill, R. E. Chrien, S. Rankowitz, B. Soucek, and O. A. Wasson, Nucl. Instr. Methods 53, 108 (1967).

[28]R. G. Greenwood, private communication with R. E. Chrien.

[29]N. C. Rasmussen, Y. Hukai, T. Inouye, and V. J. Orphan, Massachusetts Institute of Technology Nuclear Engineering Department Report No. 85 (unpublished).

[30]L. M. Bollinger and G. E. Thomas, Phys. Rev. Letters 21, 233 (1968).

[31]J. E. Draper, C. Fenstermacher, and H. L. Schultz, Phys. Rev. 111, 906 (1958).

[32]C. A. Fenstermacher, J. E. Draper, and C. K. Bockelman, Nucl. Phys. 10, 386 (1959).
[33]J. R. Huizenga and R. Vanderbosch, Phys. Rev. 120, 1035 (1960).
[34]W. P. Pönitz, Z. Physik, 197, 262 (1966).
[35]D. Sperber and J. W. Mandler, Nucl. Phys. A113, 689 (1968).
[36]K. J. Wetzel and G. E. Thomas, Phys. Rev. C 1, 1501 (1970).
[37]M. R. Bhat, R. E. Chrien, D. I. Garber, and O. A. Wasson, Phys. Rev. (to be published).
[38]M. D. Goldberg, S. F. Mughabghab, S. N. Purohit, B. A. Magurno, and V. M. May, Brookhaven National Laboratory Report No. BNL 325, 1966 (unpublished), 2nd ed., Suppl. 2.

PHYSICAL REVIEW C VOLUME 2, NUMBER 2 AUGUST 1970

Intermediate Structure in the Photon Interaction Cross Sections of Sn and Zr†

P. Axel, K. K. Min,* and D. C. Sutton
Physics Department, University of Illinois, Urbana, Illinois 61801
(Received 2 February 1970)

Photon scattering cross sections were measured with 70-keV resolution from 6 to 9 MeV in Sn, and from 8.5 to 12.5 MeV in Zr. A new method of analysis is used to infer relatively reliable total photon interaction cross sections. Both the elastic scattering and the total interaction cross sections vary more rapidly with energy than had been anticipated; the best identified localization of transition strength is between 11.4 and 11.8 MeV in Zr. The average total interaction cross sections are qualitatively similar to, but about 50% larger than, an extrapolation of the electric dipole giant resonance. The cross sections are large enough to imply that electric dipole interaction dominates at most energies. The relative probability of photon scattering and photoproton emission is very sensitive to correlations between proton widths and ground-state γ-ray widths. There is no evidence for width correlations associated with the additional strength concentrated near 11.5 MeV in ^{90}Zr.

I. INTRODUCTION

The elastic scattering of photons at energies near and below the neutron emission threshold can provide valuable new insights into several different aspects of nuclear structure. This paper will show that the observed elastic scattering can be used to obtain a reliable estimate of the total photon interaction cross section. Elastic-scattering experiments therefore make it possible to extend our knowledge of photon interactions to lower energies than can be reached with other techniques. This extension is important in order to bridge the gap between the region of the electric dipole giant resonance and very low energies which dominate nuclear γ-ray cascades.

Photon interactions in this energy region are also especially interesting because they reveal the way in which a simple nuclear excitation is shared by many neighboring complicated nuclear states. At most energies the photon cross sections measure that component of the excited states which can be reached by electric dipole absorption. Inasmuch as this component can be determined over a relatively large energy range, photon interactions should be helpful in learning more about intermediate structure.

Energy regions which consist of nonoverlapping levels have special advantages in the study of intermediate structure. Each level contributes to average cross sections in accordance with its partial widths. If one type of partial width is larger in some energy region, the levels in that region must have a larger amount of the corresponding nuclear configuration. If some nuclear configuration contributes importantly to two partial widths, these widths will be correlated. This paper will show that when photoproton emission provides the main competition for photon scattering, this scattering is exceptionally sensitive to width correlations.

Correlations between partial widths of nonoverlapping levels merit much more study than they have received. The nonoverlapping levels are well understood quasistationary quantum states whose modes of decay are independent of the modes of formation. However, the width correlations have the interesting effect of favoring some average partial cross sections disproportionately when compared with the corresponding average widths. In this sense, the correlations can be thought of as the low-energy forerunners of quasidirect, nonstatistical processes which are usually discussed as being the early temporal stages of a nuclear interaction.

There is little experimental or theoretical infor-